AMS 14th Conference on Satellite Meteorology and Oceanography
Atlanta, GA, 29 January - 2 February 2006

P2.7

SATELLITE-DERIVED SURFACE RADIATION FLUXES AT THE ARM SGP AND TWP MANUS CART SITES

Michele L. Nordeen, David R. Doelling, Pui K. Chan, Mandana M. Khaiyer,
Dung Phan, J. Kirk Ayers, and Rabindra Palikonda
Analytical Services & Materials, Inc., Hampton, Virginia

Patrick Minnis
NASA Langley Research Center, Hampton, Virginia

1. INTRODUCTION

Surface-measured radiative fluxes are important for validating climate models and assessing energy and agricultural needs. They are also potentially valuable for initializing and verifying numerical weather analysis forecasts. Since directly measured fluxes provide only minimal areal coverage, analyses of appropriate satellite data in conjunction with radiative transfer model calculations and empirical techniques are needed to provide timely and comprehensive flux estimate at all locations. A variety of techniques have been developed to convert top-of-atmosphere (TOA) albedo and outgoing longwave radiation (OLR) data to estimate up- and down-welling surface shortwave (SW) and longwave (LW) fluxes over the globe. In particular, the Clouds and Earth's Radiant Energy System (CERES) is estimating the surface radiation budget from polar-orbiting satellites using a combination of measured broadband SW and LW fluxes and cloud properties (Smith et al., 2004) retrieved from narrowband imager data (Minnis et al., 2004a). Similar methods have been applied to Geostationary Operational Environmental Satellite (GOES) narrowband data to derive such fluxes at a higher temporal resolution. Until recently, such analyses took place at some time well after the acquisition of the original satellite data because of technical difficulties and the lack of calibration of the GOES visible channels. Increases in computer speed and data transmission and the availability of calibrated visible sensors on recent satellites that can be transferred to GOES (e.g., Minnis et al., 2002), however, have eliminated those roadblocks enabling the near-real time estimation of cloud properties and TOA radiative fluxes from routine geostationary imager data (e.g., Minnis et al., 2004b). A natural extension of these products would be the estimation of surface radiative fluxes applying the methods used by CERES. In this paper, cloud and radiative products derived from GOES data over North America (Minnis et al., 2004b) and over the Tropical Western Pacific (TWP; Phan et al., 2004) to support the Atmospheric Radiation Measurement (ARM) Program are compared with direct measurements at the surface as an initial assessment of this new product. These near-real time flux parameters are being derived every 30-minutes to 1-hour over the North America and the TWP. The inferred surface fluxes are compared to fluxes measured by ARM instruments at the TWP site on Manus island and in north central Oklahoma at the ARM Southern Great Plains Central Facility (SCF).

**Corresponding author address*: Patrick Minnis, NASA Langley Research Center, MS 420, Hampton, VA 23681-2199. email: p.minnis@larc.nasa.gov.

2. DATA AND METHODOLOGIES

The cloud products were derived with the Visible Infrared Solar-infrared Split-window Technique (VISST, Minnis et al., 1995a) from radiances corresponding to 4-km pixels from GOES-9 over the TWP and from GOES-10 and GOES-12 over the SGP domain. The pixels are identified as clear or cloudy using the Clouds and Earth's Radiant Energy System (CERES) ARM Cloud Mask (CACM; Trepte et al. 2005). Broadband SW and LW TOA fluxes were derived from the visible and infrared channels, respectively, using the narrow-to-broadband conversion functions found from matching CERES broadband fluxes with the GOES data (Doelling et al. 2003, Chakrapani et al. 2003). Data from January, April, June, and October 2004 were used for the SGP site and from June and October 2003 and January and April 2004 were used for the TWP.

Several VISST parameters are used as input into three different algorithms to calculate surface fluxes. Profiles of temperature and humidity are used in both the VISST and surface flux calculations. Hourly profiles from Rapid Update Cycle (RUC; Benjamin et al. 2004) are used over the SGP and the 6-hourly Global Forecast System (GFS, formerly referred to as the Aviation forecast model, AVN) profiles are used over the TWP. Each vertical profile is temporally interpolated to match the GOES imager data for the relevant domain. Ozone concentration, aerosol optical depth (AOD), and surface emissivity data are also needed for the satellite-derived surface flux calculations. The ozone data were obtained from the Total Ozone Mapping Spectrometer (TOMS) daily climatology ozone maps (McPeters 1998). AOD data are from the Geophysical Fluid Dynamics Laboratory (GFDL) climatology and are used to calculate aerosol correction parameters for the SW flux

computations. To test the sensitivity of the fluxes to the input profile, temperature and humidity soundings from the Global Modeling Assimilation Office GEOS 4.03 (DAO, 1997) reanalyses were also used. The DAO profile is a 6-hourly profile at a 1° resolution that also provides ozone and skin temperature data. For the clear-sky flux comparisons, the average fractional sky coverages at a 15-minute resolution for both SGP and Manus were obtained from the SW Flux Analysis (CLSFA) data set to minimize points that could be cloud contaminated (Long et al. 1999). Operationally, the surface fluxes are computed from pixel-level results that are averaged over a 0.5° region. This process minimizes the processing time and smoothes the radiation field. For comparison with the surface data, TOA SW and LW fluxes were computed by using averaged values for all pixels within a 10-km radius of each surface site.

Solar Infrared Radiation Station (SIRS) 1-minute data, obtained from the *sgpsirs* files in the ARM archive, are used to validate the satellite-derived surface fluxes over the SGP. At the SGP CF, 10-minute means centered on the satellite image time were computed from the 1-minute SIRS data. Over the TWP, the same process is used, except that the ARM groundrad (GRAD) and skyrad (SRAD) measurements replace the SIRS data. The TWP CART site ground radiometer b1 files (*twpgndrad60s* or *twpskyrad60s*) were obtained from the ARM archive. The *twpgndrad60s* files contain the upwelling SW and LW hemispheric irradiances from the pyranometer and pyrgeometer, respectively. The *twpskyrad60s* files contain the downwelling SW and LW hemispheric irradiances from the pyranometer and the shaded pyrgeometer1, respectively.

The Li-Leighton (LL) method is used to compute the downward surface SW flux only in clear-sky conditions (Li et al. 1993). This technique requires the following inputs: AOD, cosine of the solar zenith angle (csza), precipitable water, and TOA SW albedo. For the comparisons, both the CACM cloud fraction and the cloud fraction from the CLSFA are used to determine clear-sky conditions. The maximum cloud fraction allowed for selecting clear-sky conditions is 5%.

The NASA Langley Parameterized Shortwave Algorithm (LPSA) method is used to estimate surface SW downwelling flux under all-sky conditions (Gupta et al. 2001) and surface albedo in clear-sky conditions. This technique uses precipitable water, ozone, AOD, humidity profiles, csza, TOA clear-sky and cloudy SW albedo, cloud fraction and Earth Radiation Budget Experiment (ERBE) scene type. To compare the LPSA SW results with surface radiation measurements, the results are divided into clear-sky and cloudy conditions using the CACM cloud fraction. For clear-sky conditions, both the CACM cloud fraction and the CLSFA cloud fraction must be less than or equal to 5% and cloudy conditions must have a CACM cloud fraction greater than 5%.

The NASA Langley Parameterized Longwave Algorithm (LPLA) method is used to estimate surface LW fluxes. The LPLA uses a set of parameterizations to compute surface LW upwelling and downwelling fluxes under all-sky conditions (Gupta et al. 1992). Inputs to this algorithm are liquid and ice cloud emissivity, cloud fraction, liquid and ice cloud base pressures, surface emissivity, and sounding profiles. As with the SW surface results the LW flux results are divided into clear-sky and cloudy conditions when comparing with surface radiation measurements based on the CACM and CLSFA cloud fraction.

3. RESULTS AND DISCUSSION

Figure 1 shows an example of the cloud phase (Fig. 1a) derived from GOES-10 and GOES-12 over the North American domain along with the downwelling LW (Fig. 1b) and SW (Fig. 1c) estimated using the LPLA and LPSA, respectively. The downwelling SW fluxes appear to decrease with latitude in the clear regions while the downwelling LW fluxes are greatest over the cloudy regions as expected. These values are computed every half hour using near-real time cloud and TOA flux retrievals over North America and the TWP.

The LPSA-derived clear-sky SW downwelling flux over the SCF underestimates the SIRS SW downwelling flux by an average of 5.3 Wm^{-2} or less than 1% (Fig. 2). The underestimate is greatest at the higher values and becomes an overestimate at the low end of the scale. Overall, the LPSA RMS error is 8.3% for the clear-sky cases. Table 1 summarizes the validation results for the SW fluxes calculated over the SCF and Manus sites. A positive bias indicates that the satellite-derived surface flux overestimates the observed flux and a negative bias indicates underestimation. Under clear-sky conditions, both sites underestimate the SW downwelling fluxes with the LL method yielding a slightly larger bias (-2.2%) over the SGP and a considerably smaller bias (-3%) than the LPSA (-6.5%) over Manus. In cloudy conditions, each site overestimates the SW downwelling fluxes during cloudy conditions. The larger biases and RMS differences over Manus could be due to its coastal location, which could cause large uncertainties in the true cloud amounts and surface albedo affecting the direct measurements. The bias over the SCF for clear-sky conditions is close to that observed over the same site by CERES (http:// snowdog.larc.nasa.gov/cave/ cave2.0/Ancil.dir/valplot/) using more sophisticated radiative transfer calculations and directly measured broadband SW radiances. However, the RMS errors are much larger in the current retrieval. The CERES retrievals over Manus are also similar to the present results in bias and in the RMS differences.

At the SFC, the downwelling LW flux (DLW) in clear skies (Table 2) is underestimated by 15 Wm^{-2} during the day using the RUC profiles, but only by 5 Wm^{-2} at night.

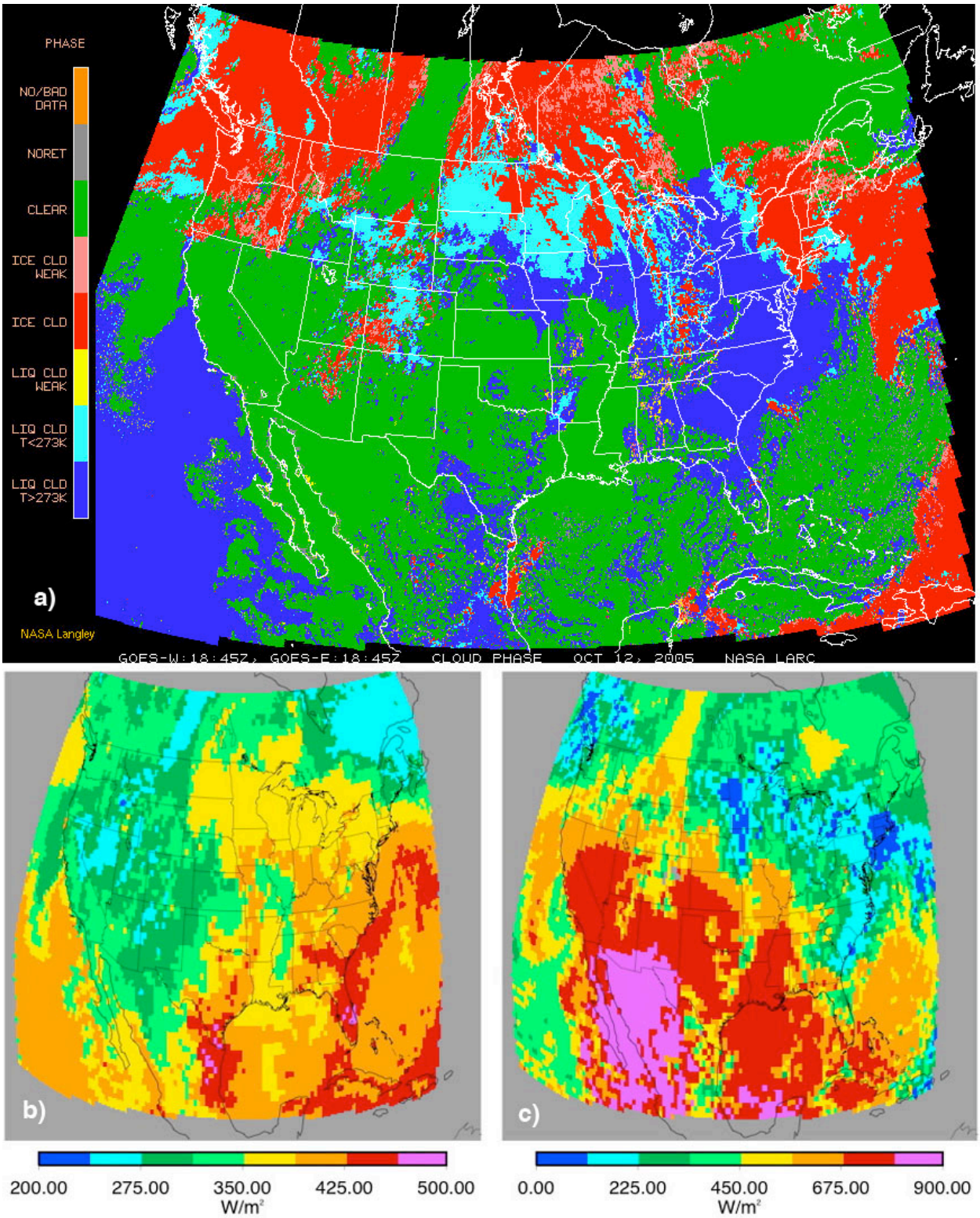

Figure 1. Cloud and surface radiation parameters over North America derived from GOES-10 and 12, 1845 UTC, 12 October 2005. (a) Cloud phase, (b) LPLA downwelling LW flux, (c) LPSA downwelling SW flux for all sky conditions.

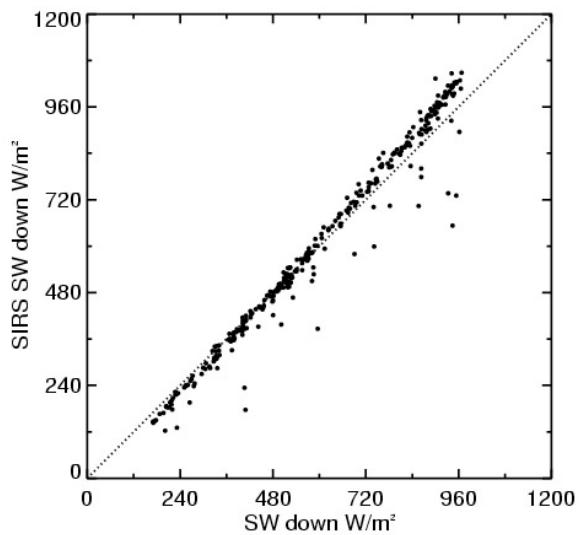

Figure 2. *Comparison of satellite-derived SW downwelling flux from LPSA with SW downwelling surface flux over the SCF under clear-sky conditions.*

Since downwelling LW clear-sky flux is a function of the 800-1000 hPa temperature and humidity profile, the differences in the calculated fluxes are highly dependent on the profile used. Using the DAO data at the SCF reduces the clear-sky biases to negligible levels during the day and night. Over Manus during the day, clear DLW is too high by 10 Wm^{-2} (2%) using the GFS, but is unbiased at night. The biases are around 1% or less using the DAO.

The upwelling LW flux (ULW) at the surface is basically the surface emissivity multiplied by the Stefan-Boltzmann function of the skin temperature. Although skin temperature is computed internally in the VISST cloud products for clear scenes, it is not currently saved as output. Thus, for this paper, the skin temperature is estimated from the RUC and GFS air temperature using the correction equation of Minnis et al. (1995b). The DAO includes an estimate of skin temperature. In cloudy conditions, the surface air temperature is assumed to be equal to the skin temperature. These different approaches to estimating skin temperature are a likely

Table 1. Summary of differences in satellite-derived SW surface fluxes over the SCF and Manus where clear-sky conditions are represented as clr and cloudy conditions as cld.

Method	SCF			Manus		
	BIAS (Wm^{-2})	RMS (Wm^{-2})	RMS (%)	BIAS (Wm^{-2})	RMS (Wm^{-2})	RMS (%)
LL (clr)	-13.9	47.9	7.91	-21.2	78.1	11.7
LPSA (clr)	-5.3	50.0	8.3	-43.5	93.8	14.1
LPSA (cld)	20.7	91.0	27.0	26.0	164.6	36.8

Table 2. Summary of differences in LPLA-derived LW surface fluxes. Daytime downwelling fluxes for clear and cloudy conditions are denoted as dclr↓ and dcld↓, respectively. Nighttime downwelling fluxes for clear-sky and cloudy conditions are denoted as nclr↓ and ncld↓, respectively. LW upwelling fluxes are indicated with an up arrow (↑).

Method	SCF RUC			SCF DAO		
	BIAS (Wm^{-2})	RMS (Wm^{-2})	RMS (%)	BIAS (Wm^{-2})	RMS (Wm^{-2})	RMS (%)
LPLA (dclr↓)	-15.2	17.4	6.6	3.5	11.1	4.5
LPLA (dcld↓)	25.4	29.5	9.3	16.6	22.1	6.8
LPLA (nclr↓)	-3.9	7.7	3.1	-1.1	8.8	3.6
LPLA (ncld↓)	5.9	26.1	8.1	9.5	26.7	8.3
LPLA (dclr↑)	0.4	8.8	2.3	-13.8	22.9	6.1
LPLA (dcld↑)	12.9	21.1	5.6	4.3	17.3	4.5
LPLA (nclr↑)	-1.5	10.3	3.3	10.2	18.0	5.7
LPLA (ncld↑)	-5.6	10.0	2.8	7.7	14.8	4.2
	Manus GFS			Manus DAO		
LPLA (dclr↓)	10.1	15.1	3.6	-1.4	5.3	1.3
LPLA (dcld↓)	23.7	27.2	6.3	0.8	9.9	2.3
LPLA (nclr↓)	0.8	8.7	2.1	4.1	9.0	2.2
LPLA (ncld↓)	6.8	11.9	2.8	7.2	11.8	2.8

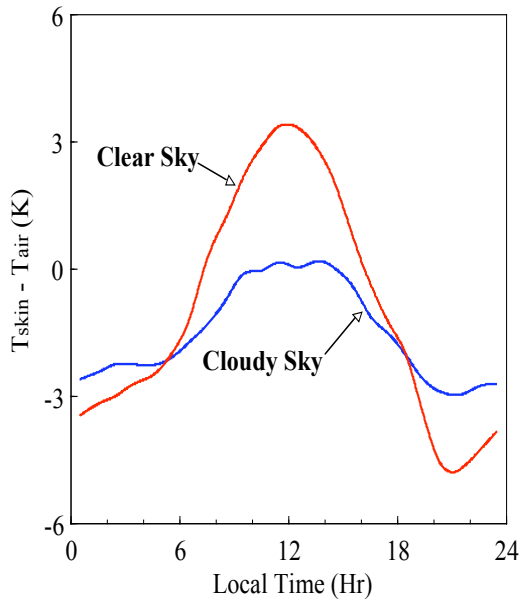

Figure 3. Hourly mean differences between skin and air temperatures over the SCF for the study period.

source of error for the present study. Only the RUC upwelling data are shown in Table 2 since the coastal placement of the radiometers at Manus will produce dramatically different results compared to the satellite which views portions of the sea and land in a single pixel. Over the SCF, the RUC-based values of ULW in clear skies are relatively unbiased but, with the DAO, are too small by 14 Wm^{-2} during the daytime and too large by 8 Wm^{-2}.

When clouds are present, the RUC-based calculations overestimate the daytime flux and underestimate the nighttime ULW. The mean bias from DAO is 6 Wm^{-2} and positive during the day and at night. The RUC results suggest that the surface air temperature is not sufficient to serve directly as the skin temperature in cloudy skies, while the DAO results indicate that the skin temperature is slightly overestimated in cloudy skies at all times at the SCF. Figure 3 shows the average difference between the skin and air temperatures at the SCF based on the surface data. It indicates that, on average, the air and skin temperature vary in a manner similar to that predicted using the correction curve in clear skies, but that the skin is colder than the air during most of the day when it is cloudy. A small error in the surface emissivity would shift the curve up or down resulting in the sort of day-night difference seen for the RUC-based results.

In cloudy skies, DLW is affected by the cloud base temperature as well as the temperature and humidity profiles. Here, the cloud base pressure was derived from the parameterization of Chakrapani et al. (2002). During the daytime, the DLW is too high by 25 and 17 Wm^{-2} using the RUC and DAO, respectively, over the SFC. At night, the errors are reduced considerably for both input models suggesting that the cloud base heights are estimated better at night than during the daytime. The results for the GFS over Manus are similar to those for the RUC. The DLW computed over Manus during the day is nearly unbiased using the DAO. In the Tropics the DLW is mostly affected by the moisture in the low layers, so any errors in cloud-base pressure are likely to have less influence than over the SCF. Thus, it appears that the DAO provides a better characterization of the temperature and humidity fields than either of the other models over the locations studied here.

The overestimation of DLW in cloudy skies over the SCF is in opposition to that determined by CERES which underestimates the overcast DLW 12 Wm^{-2}. Similarly, CERES underestimates the overcast DLW by 3 W m^{-2} over Manus, on average, compared to the 4 Wm^{-2} overestimate using the DAO here. The source of the differences will require further study.

4. SUMMARY AND FUTURE WORK

The preliminary results presented here indicate that, except for DLW in cloudy skies, the methodologies applied to the VISST cloud and radiation products produce estimates of surface radiation fields that are nearly as accurate as those derived using directly measured broadband radiation and sophisticated calculation methods. However, additional study of the differences and refinement of the input data are needed to reduce the errors, especially in for DLW in cloud conditions. The satellite-derived surface temperature should be used in clear conditions and a more sophisticated method of estimating skin temperature in cloudy conditions should be developed. The narrow-to-broadband conversion functions should be optimized for each location and season to provide the best estimates of TOA fluxes with subsequent improvement of the surface estimates. Further study of the input model profiles should be performed to employ the best techniques for minimizing errors in the near-real time products. With the implementation of these improvements, the surface radiation budget will become part of the operational near-real time VISST products.

5. ACKNOWLEDGEMENTS

The radiometer and surface temperature data were obtained from the ARM Program sponsored by the U.S. Department of Energy, Office of Science, Office of Biological and Environmental Research, Environmental Sciences Division. The atmospheric profiles were generated by the CERES Meteorological, Ozone, and Aerosols group and obtained from the NASA Langley Atmospheric Sciences Data Center. This research was sponsored by ITF No. 214216-A-Q1 from Pacific Northwest National Laboratory, and Environmental Sciences Division of the U.S. Department of Energy Interagency Agreement DE-AI02-97ER62341.

6. References

Benjamin, SG, D Dévényi, SS Weygandt, KJ Brundage, JM Brown, GA Grell, D Kim, BE Schwartz, TG Smirnova, TL Smith, GS Manikin. 2004 "An hourly assimilation-forecast cycle: The RUC." *Monthly Weather Review* 132, 495-518.

Chakrapani, V., D. R. Doelling, M. M. Khaiyer, and P. Minnis, 2003: New visible to broadband shortwave conversions for deriving albedos from GOES-8 over the ARM SGP. *Proc. 13th ARM Science Team Meeting*, Broomfield, CO, March 31 - April 4.

Chakrapani, V., D. R. Doelling, A. D. Rapp, and P. Minnis, 2002: Cloud thickness estimation from GOES-8 satellite data over the ARM SGP site. *Proc. 12th ARM Science Team Meeting*, April 8-12, St. Petersburg, FL, 14 pp.

DAO, 1997: GEOS-3 Data Assimilation System Architectural Design. *DAO Office Note 97-06*. Data Assimilation Office, Goddard Space Flight Center, Greenbelt, MD 20771.

Doelling, D. R., M. L. Nordeen, M. M. Khaiyer, and P. Minnis, 2003: Improved ARM-SGP OLR fluxes from GOES-8 based on CERES. *Proc. 13th ARM Science Team Meeting*, Broomfield, CO, March 31 - April 4.

Gupta, S. K., W. L. Darnell, A. C. Wilber, 1992: A parameterization for longwave surface radiation from satellite data: Recent improvements. *J. Appl. Meteorol.,* **31**, 1361-1367

Gupta, S. K.,D. P. Kratz, P. W. Stackhouse, Jr. and A. C. Wilber, 2001: *The Langley Parameterized Shortwave Algorithm (LPSA) for Surface Radiation Budget Studies---Version 1.0*, NASA/TP-2001-211272, p. 26.

Li, Z., H. G. Leighton, K. Masuda, and T. Takashima, 1993: Estimation of SW Flux Absorbed at the Surface from TOA Reflected Flux. *J. Climate*, **6**, 317-330.

Long, C. N. and K. L. Gaustad, (2001/2004): The shortwave (SW) clear-sky detection and fitting algorithm: Algorithm operational details and explanations. Atmospheric Radiation Measurement Prog. Tech. Rpt., *ARM-TR-004.1*, http://www.arm.gov/publications/tech_reports/vaps.stm

Long, C. N. and T. P. Ackerman, 2000: Identification of clear skies from broadband pyranometer measurements and calculation of downwelling shortwave cloud effects. *J. Geophys. Res.*, **105**, 15609-15626.

Long, C. N., T. P. Ackerman, J. J. DeLuisi, and J. Augustine, 1999: Estimation of fractional sky cover from broadband SW radiometer measurements. *Proc. 10th Conf. on Atmos. Rad.*, June 28-July 2, 1999, Madison, Wisconsin.

Minnis, P., and Co-authors, 1995a: Cloud Optical Property Retrieval (Subsystem 4.3). "Clouds and the Earth's Radiant Energy System (CERES) Algorithm Theoretical Basis Document, Volume III: Cloud Analyses and Radiance Inversions (Subsystem 4)", *NASA RP 1376 Vol. 3*, edited by CERES Science Team, pp. 135-176.

Minnis, P., L. Nguyen, D. R. Doelling, D. F. Young, W. F. Miller, and D. P. Kratz, 2002: Rapid calibration of operational and research meteorological satellite imagers, Part I: Evaluation of research satellite visible channels as references. *J. Atmos. Oceanic Technol.*, **19**, 1233-1249.

Minnis, P., L. Nguyen, W. L. Smith, Jr., M. M. Khaiyer, R. Palikonda, D. A. Spangenberg, D. R. Doelling, D. Phan, G. D. Nowicki, P. W. Heck, and C. Wolff, 2004b: Real-time cloud, radiation, and aircraft icing parameters from GOES over the USA. *Proc. 13th AMS Conf. Satellite Oceanogr. and Meteorol.*, Norfolk, VA, Sept. 20-24, CD-ROM, P7.1.

Minnis, P., W. L. Smith, Jr., D. P. Garber, J. K. Ayers, and D. R. Doelling, 1995b: Cloud properties derived from GOES-7 for the Spring 1994 ARM Intensive Observing Period using Version 1.0.0 of the ARM satellite data analysis program. *NASA RP 1366*, 59 pp.

Minnis, P., D. F. Young, S. Sun-Mack, Q. Z. Trepte, R. R. Brown, S. Gibson, and P. Heck, 2004a: Diurnal, seasonal, and interannual variations of cloud properties derived for CERES from imager data. *Proc. 13th AMS Conf. Satellite Oceanogr. and Meteorol.*, Norfolk, VA, Sept. 20-24, CD-ROM, P6.10.

McPeters, RD, PK Bhartia, AJ Krueger, JR Herman, CG Wellemeyer, CJ Seftor, G Jaross, O Torres, L Moy, G Lavow, W Byerly, SL Taylor, T Swissler, and RP Cebula. 1998. Earth Probe Total Ozone Mapping Spectrometer (TOMS) Data Products User's Guide. NASA Reference Publication 1998-206895

Phan, D, DA Spangenberg, R Palikonda, MM Khaiyer, ML Nordeen, L Nguyen, and P Minnis. 2004. "Web-based satellite products database for meteorological and climate applications." In Proceedings of the Thirteenth AMS Conference Satellite Oceanography and Meteorology, Norfolk, Virginia, September 20-24, CD-ROM, P8.2.

Smith, G. L., B. A. Wielicki, B. R. Barkstrom, R. B. Lee, K. J. Priestley, T. P. Charlock, P. Minnis, D. P. Kratz, and N. Loeb, 2004: Clouds and Earth Radiant Energy System (CERES): An overview. *Adv. Space Res.*, **33**, 1125-1131.

Trepte, QZ, P Minnis, PW Heck, and R Palikonda. 2005. "Improvements in near-terminator and nocturnal cloud masks using satellite imager data over the ARM sites." In Proceedings of the Fifteen ARM Science Team Meeting, Daytona Beach, Florida, March 14-18.